Journal of Pharmaceutical Sciences 107 (2018) 317-326

Contents lists available at ScienceDirect

Journal of Pharmaceutical Sciences

journal homepage: www.jpharmsci.org

Pharmaceutics, Drug Delivery and Pharmaceutical Technology

Moisture-Induced Amorphous Phase Separation of Amorphous Solid Dispersions: Molecular Mechanism, Microstructure, and Its Impact on Dissolution Performance

Huijun Chen [1], Yipshu Pui [1], Chengyu Liu [1], Zhen Chen [1], Ching-Chiang Su [2], Michael Hageman [3], Munir Hussain [4], Roy Haskell [5], Kevin Stefanski [2], Kimberly Foster [2], Olafur Gudmundsson [2], Feng Qian [1, *]

[1] School of Pharmaceutical Sciences and Collaborative Innovation Center for Diagnosis and Treatment of Infectious Diseases, Tsinghua University, Beijing, China
[2] Pharmaceutical Candidate Optimization, Bristol-Myers Squibb Company, Lawrenceville, New Jersey 08648
[3] Department of Pharmaceutical Chemistry, University of Kansas, 2095 Constant Avenue, Lawrence, Kansas 66047
[4] Drug Product Science and Technology, Bristol-Myers Squibb Company, New Brunswick, New Jersey 08901
[5] Pharmaceutical Candidate Optimization, Bristol-Myers Squibb Company, Wallingford, Connecticut 06492

ARTICLE INFO

Article history:
Received 4 August 2017
Revised 11 October 2017
Accepted 17 October 2017
Available online 26 October 2017

Keywords:
amorphous
solid dispersion
physical stability
drug-excipient interaction
dissolution rate

ABSTRACT

Amorphous phase separation (APS) is commonly observed in amorphous solid dispersions (ASD) when exposed to moisture. The objective of this study was to investigate: (1) the phase behavior of amorphous solid dispersions composed of a poorly water-soluble drug with extremely low crystallization propensity, BMS-817399, and PVP, following exposure to different relative humidity (RH), and (2) the impact of phase separation on the intrinsic dissolution rate of amorphous solid dispersion. Drug-polymer interaction was confirmed in ASDs at different drug loading using infrared (IR) spectroscopy and water vapor sorption analysis. It was found that the drug-polymer interaction could persist at low RH ($\leq$75% RH) but was disrupted after exposure to high RH, with the advent of phase separation. Surface morphology and composition of 40/60 ASD at micro-/nano-scale before and after exposure to 95% RH were also compared. It was found that hydrophobic drug enriched on the surface of ASD after APS. However, for the 40/60 ASD system, the intrinsic dissolution rate of amorphous drug was hardly affected by the phase behavior of ASD, which may be partially attributed to the low crystallization tendency of amorphous BMS-817399 and enriched drug amount on the surface of ASD. Intrinsic dissolution rate of PVP decreased resulting from APS, leading to a lower concentration in the dissolution medium, but supersaturation maintenance was not anticipated to be altered after phase separation due to the limited ability of PVP to inhibit drug precipitation and prolong the supersaturation of drug in solution. This study indicated that for compounds with low crystallization propensity and high hydrophobicity, the risk of moisture-induced APS is high but such phase separation may not have profound impact on the drug dissolution performance of ASDs. Therefore, application of ASD technology on slow crystallizers could incur low risks not only in physical stability but also in dissolution performance.

Introduction

Advances in combinatorial chemistry and high-throughput screening have given rise to increasing amount of poorly water-soluble drugs in drug discovery.[1] The appearance of amorphous solid dispersions (ASDs) has provided a promising formulation strategy to increase the dissolution rate and solubility of poorly water-soluble compounds thus to improve the oral bioavailability.[2-6] As high energy and metastable binary systems where drug molecules disperse in polymer matrix above crystalline drug solubility,[7] one of the major physical stability concerns of ASDs is amorphous drug recrystallization into a thermodynamically more stable crystalline form, thus diminishing the solubility advantage of amorphization. At the same time, ASDs could also undergo amorphous phase separation (APS), either due to suboptimized processing conditions

* *Correspondence to:* Feng Qian (Telephone: 86-10-62794733; Fax: 86-10-62771859).
E-mail address: qianfeng@biomed.tsinghua.edu.cn (F. Qian).

https://doi.org/10.1016/j.xphs.2017.10.028
0022-3549/

or aging during storage,[8-10] to produce drug-rich and polymer-rich domains, wherein drug still remains amorphous. For poorly water-soluble drugs that crystallize relatively slow, the risk of APS could be dominant, especially considering most of these drugs are highly lipophilic (i.e., high risk of phase separation from hydrophilic carriers but without crystallization), whereas the presence of moisture serves as an unavoidable APS catalyst.

Moisture-induced APS was reported in many ASD systems prepared by drugs and polymers with various physicochemical properties, including nifedipine-PVP, droperidol-PVP, and pimozide-PVP, felodipine-PVPVA, pimozide-PVPVA, and pimozide-HPMCAS and so forth.[9-13] When sorbed water penetrates into ASDs, water molecules could overtake the drug molecules to form new hydrogen bonding with polymers, destroy the original drug-polymer interaction and render it thermodynamically immiscible.[9,13] At the same time, water also acts as a strong plasticizer to significantly decrease the glass transition temperature (T_g) and increase the molecular mobility of ASDs.[14-16] These 2 mechanisms could be driving the moisture-induced APS indistinguishably and synergistically.

It is generally assumed that in a miscible ASD system, amorphous drug disperses in the polymer matrix at molecular level, and polymer stabilizes the amorphous drug by decreasing the molecular mobility through specific or nonspecific drug-polymer interactions.[7,17,18] Meanwhile, the drug-polymer interaction was also believed to be a key mechanism behind the improved drug supersaturation in solution with the presence of polymers.[19,20] In addition, hydrophilic polymer carrier could also increase the wettability and dispersability of the hydrophobic amorphous drug during dissolution by surrounding and interacting with it intimately.[21] Therefore, the potential impacts of the disruption of drug-polymer interactions and APS on the physical stability and dissolution performance of ASD could be catastrophic, and the risk of APS is certainly worth attention during ASD formulation development.

Previous studies on APS have been focusing on the factors affecting the apparent tendency and kinetics of APS on exposure to moisture.[10-13,22] For instance, it was concluded that weaker drug-polymer interactions, high ASD hygroscopicity, and more hydrophobic APIs, were reasons behind ASDs susceptible to moisture-induced APS.[10] It was also reported that the rate of ASD phase separation depended on the initial drug content and drug-polymer interactions.[13] APS was also reported to be related with accelerated crystallization kinetics of amorphous drugs in a number of systems,[11] wherein much earlier onset of drug crystallization was observed in pimozide-PVP, and 2 other systems exhibiting phase separation when compared to indomethacin/PVP system that remained homogenously mixed.[11]

Although moisture-induced phase separation kinetics and phase behaviors of ASDs have been extensively studied, knowledge about its molecular mechanism, microstructure, and the explicit consequence on the intrinsic dissolution rate of ASDs is still lacking. While it is generally considered that crystallization will inevitably negate the solubility advantage of amorphous drugs, the impact of APS on the dissolution rate of ASDs and subsequent supersaturation maintenance has not been clearly studied so far. Previously, we compared the intrinsic dissolution performance of ASDs with good uniformity, and physical mixtures with the same overall drug content but mixed by ASDs with high and low drug loading (i.e., artificially prepared ASD systems with APS), and the results suggested that changes in the mixing state of ASDs could affect the dissolution behavior of ASDs to different extents, largely depending on the strength of drug-polymer interactions.[23] The artificially prepared ASDs with APS could certainly be very different in their microstructure and dissolution performance, compared with ASDs with moisture-induced APS, which are real-life scenarios. Therefore, in this study, we aim to (1) investigate the effect of moisture on the drug-polymer interaction and microstructure of a model ASD system based on BMS-817399, a lipophilic slow crystallizer, and PVP, a commonly used hydrophilic polymer; (2) to study the impact of APS on the intrinsic dissolution rate of both the drug and polymer from ASDs.

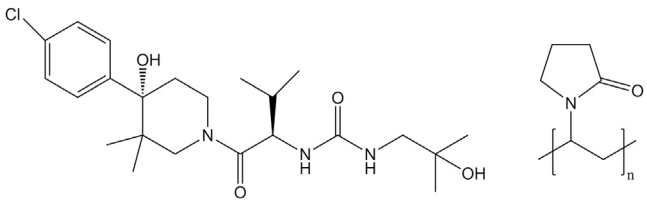

Figure 1. Chemical structures of model compound and polymer.

Materials and Methods

Materials

BMS-817399 was obtained from BMS (Bristol-Myers Squibb). BMS-817399 is a poorly water-soluble, nonionizable (pH 2-11) drug with a melting point of 210°C, a glass transition temperature of 116°C, water solubility of 40 μg/mL, and Log D (pH 6.5) = 3.26. PVP K30 (Kollidon) was provided by BASF Chemical Company Ltd. (Ludwigshafen, Germany). PVP was used as a model polymer here because PVP is widely used in ASDs, and it also forms specific interactions with BMS-817399 (shown below). Moreover, PVP was selected due to its high hygroscopicity, which facilitated the investigation on moisture-induced APS in ASDs. The chemical structures of BMS-817399 and PVP were shown in Figure 1. All buffer salts used for dissolution medium, as well as methanol (high-performance liquid chromatography [HPLC] grade) were obtained from Beijing Chemical Works (Beijing, China).

Preparation of BMS-817399/PVP Amorphous Solid Dispersions Using Spray Drying

The amorphous solid dispersions were prepared by spray drying (B-90; Büchi Labortechnik AG, Postfach, Switzerland). Pure BMS-817399 and drug-polymer blends with 20, 40, 60, and 80 wt % drug were dissolved in methanol with a total concentration of 5 wt %, and then the solution was spray-dried using the following conditions: inlet temperature 80°C, outlet temperature 50°C-53°C, N_2 flow rate of 100 L/min. After spray drying, materials were collected and vacuum-dried for 24 h, and then stored at 4°C for further use. The solid dispersions were confirmed to be amorphous by powder X-ray diffraction (PXRD) and polarized microscope (data not shown). Physical mixture (PM) with 20, 40, 60 and 80 wt % drug loading were prepared by PVPK30 and pure amorphous BMS-817399 prepared by spray drying. Another physical mixture with a total 40% drug loading was also prepared by mixing 2 spray dried ASDs with 20% and 60% drug loading, respectively.

Powder X-Ray Diffraction

PXRD patterns of the samples from 5° to 45° (2θ) were collected by a PANalytical X' pert Powder X-ray Diffractometer (copper X-ray tube, 40 kV × 40 mA; PANalytical, Almedo, The Netherlands), at a speed of 8°/min, with automatic divergence slit graphite monochromator, 0.2 mm receiving slit.

Fourier Transform Infrared Spectrum

Fourier transform infrared (FT-IR) spectra of pure amorphous BMS-817399, PVP, and ASDs in the range of 4000-600 cm^{-1} with a spectral resolution of 4 cm^{-1} were collected by FT-IR (Vertex 70; Bruker Optics, Ettlingen, Germany). FT-IR spectra of ASDs after water vapor sorption experiment were also obtained using the same settings.

Modulated Differential Scanning Calorimeter

The glass transition temperature (T_g) of the solid dispersions was measured by differential scanning calorimetry (DSC) (TA DSC Q2000; TA Instruments, New Castle, DE). Briefly, 5-10 mg of ASD samples was loaded into pin-holed, crimped aluminum pans. The sample was first heated to 105°C and maintained for 3 min to remove any residual solvent or water and scanned at 2°C/min from 40°C to 170°C with an amplitude of ±0.5°C and a period of 60 s (degradation was found when heating to higher than 170°C, data not shown).

Water Vapor Sorption

To study the drug-polymer interaction, water vapor sorption isotherms of pure amorphous drug, PVP, and ASDs under different relative humidities (RH) were measured using DVS instrument (Surface Measurement Systems, London, UK). Before the sorption run, all the samples were first held at 0% RH to equilibrium to remove the water content sorbed during environmental exposure in storage or sample loading. The samples were then subjected to a stepwise change of relative humidity from 3% to 33% RH in steps of 5% RH. The humidity was adjusted to the next RH level after 360 min or if the equilibrium criterion had been met. Equilibrium was assumed to be achieved if the mass change per minute was less than 0.002% over 10 min. All the water vapor sorption experiments were performed at 298 K. At the end of the sorption run, all the samples were dried at 0% RH until dm/dt <0.002% per min for 10 min and then checked for crystallinity using PXRD.

To study the phase behavior of ASDs, ASD samples weighed 8-15 mg were subjected to a jump run from 0% RH to certain targeted RH for 360 min at 298 K to reach equilibrium and exclude the influence of equilibrium time on the phase separation. Again, all samples were immediately dried at 0% RH after the water sorption and confirmed to be amorphous by XRD. FT-IR or DSC analysis was performed afterward to determine the phase behaviors of ASDs after moisture exposure. For 40/60 ASD, a second stepwise run using same settings as abovementioned was also performed to study the drug-polymer interaction after exposure to different RH.

Scanning Electron Microscopy

The surface morphologies of 40/60 ASD powders before and after 95% RH exposure were analyzed using a scanning electron microscope (FEI Quanta 200; FEI, Eindhoven, the Netherlands) operated at an excitation voltage of 15 kV. Samples were mounted onto copper stage and coated with gold before observation.

X-Ray Photoelectron Spectroscopy

The surface chemical composition of 40/60 ASD before and after 95% RH exposure was determined using X-ray photoelectron spectra. X-Ray photoelectron spectroscopy (XPS) were performed on the ESCALab 250Xi (Thermo Scientific) with a 6 channeltron hemispherical sector analyzer under a base pressure of 1×10^{-7} mbar in the analysis chamber, using 200 W monochromatic Al Ká radiation. The X-ray spot size for analysis was 500 μm, and C 1s line at 284.8 eV from adventitious carbon was used for energy referencing. All spectra analysis and curve fitting were performed using the Avantage Software (Thermo). The fraction of BMS-817399 and PVP on the surface of ASD powders was calculated based on the surface atomic percentage of the Cl element in the BMS-817399 and N element in both BMS-817399 and PVP.

Intrinsic Dissolution

Tablets of 40/60 (w/w) ASD before and after 95% RH exposure were prepared using a press (Focs Analysis Instrument, Shanghai, China) at a pressure of 100 kgf with a diameter of 8 mm. Only one surface of the tablets was exposed to the dissolution medium. The intrinsic dissolution of obtained tablets was carried out using an United States Pharmacopeia II apparatus (Focs Analysis Instrument) under sink conditions, with a dissolution medium of 500 mL of 50-mM PBS at 37°C and a rotation speed of 300 rpm. A 4-mL dissolution solution was withdrawn at each time point and filtered with 0.45 μm syringe filter. A 0.5-mL solution was used for drug concentration measurement while the remaining 2-mL solution was freeze-dried and reconstituted in 200-μL methanol to measure the PVP concentration. The concentration of API in the dissolution medium was analyzed by HPLC (Shimadzu LC-20AT; Shimadzu, Kyoto, Japan) with a XTerra MS C18 column (5 μm, 4.6 × 150 mm) and a UV−*vis* spectrophotometer. The mobile phase consisting of acetonitrile (A) and water (B) (45:55, v/v), was pumped at a flow rate of 1.0 mL/min at 30°C. The injection volume was 10 μL, and the detecting wavelength was 220 nm. The concentration of PVP after reconstitution was measured by HPLC (1260 series; Agilent Technologies, Santa Clara, CA) with a RSpak DS-413 polystyrene gel column (3.5 μm, 4.6 × 150 mm; Shodex, Tokyo, Japan) and an evaporative light scattering detector (ELSD). The mobile phase was acetonitrile (A) and water (B), both containing 0.1% formic acid and the injection volume was 50 μL. A gradient elution starting at 72% B and 28% A was run to separate salts, drug, and PVP chromatographically, at a flow rate of 0.5 mL/min. The polymer concentration was determined based on the calibration curve of ELSD scattering intensity versus polymer concentration. The intrinsic dissolution rate was calculated using the slope of concentration-time plot.

Crystallization Propensity of Amorphous BMS-817399

Polarized light microscopy (PLM, Zeiss Axio Imager A2m; Carl Zeiss, Berlin, Germany) was used to study the crystallization kinetics of amorphous BMS-817399 film when encountering moisture. Briefly, amorphous film of BMS-817399 was prepared by solvent evaporation and vacuum drying for 24 h. It was confirmed to be amorphous using PLM before moisture exposure. The amorphous film was then stored at 97% RH in a desiccator with saturated K_2SO_4 salt solution at ambient temperature and checked for crystallinity at set intervals using PLM.

Supersaturation Kinetics of BMS-817399 in Aqueous Solution

The ability of amorphous BMS-817399 to maintain supersaturation in aqueous solution with or without PVP was assessed using prior reported protocols.[19] Briefly, 100 μL of drug solution in dimethyl sulfoxide was added to 20-mL 50-mM PBS dissolution medium (pH = 6.5) with or without predissolved PVP (1.5 or 0.6 mg/mL) to generate an initial supersaturation of 1 or 0.4 mg/mL. The concentration of PVP was selected to generate an initial BMS-817399/PVP concentration ratio of 40/60. The solution was then vibrated at 100 rpm, 37°C in a Burrell wrist action shaker. After 0.25, 0.5, 1, 2, and 4 h, 300-μL solution was withdrawn and centrifuged (13000 rpm) for 3 min, and the drug concentration in the supernatant was analyzed using HPLC (Shimadzu LC-20AT;

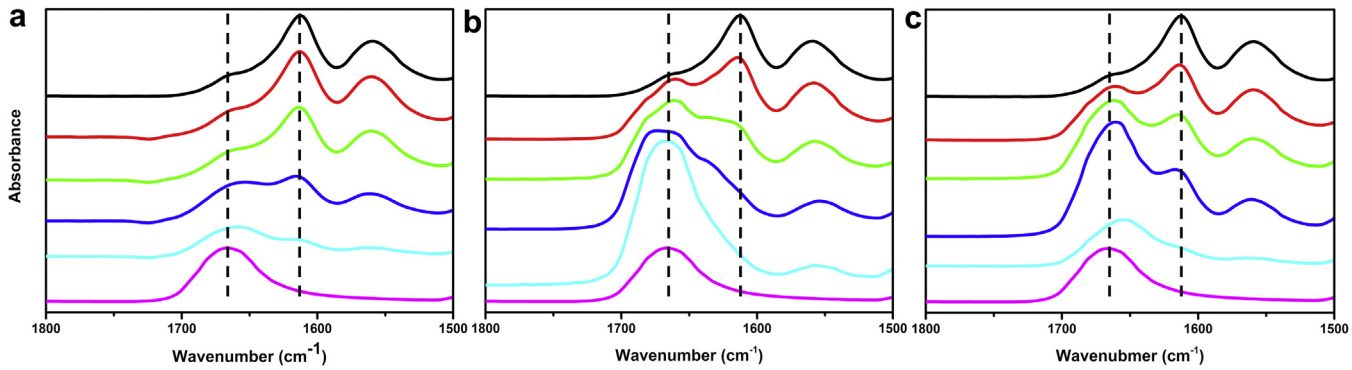

Figure 2. FT-IR spectra of the carbonyl groups of BMS-817399/PVP PMs (a) and BMS-817399/PVP ASDs at different drug loadings before (b) and after (c) 95% RH exposure. Drug loading in each figure was 100% (pure amorphous BMS-817399), 80%, 60%, 40% 20%, and 0% (pure PVPK30), from top to bottom respectively. The left dash line in each figure indicated the carbonyl group of PVP, whereas the right one indicated the carbonyl group of pure amorphous BM-817399.

Shimadzu). For comparison, the solubility of crystalline BMS-817399 in the dissolution medium was also determined.

Results and Discussion

Specific Drug-Polymer Interactions Studied by FT-IR

Drug-polymer interaction is considered to be necessary for complete miscibility and also helpful for physical stability of ASDs.[7,17,18] Strong drug-polymer interaction could prevent moisture-induced phase separation in ASDs thus to make them moisture resistant.[10,13] Drug-polymer interaction also plays an important role during the dissolution process of ASDs.[19,23,24] Therefore, the molecular interaction between BMS-817399 and PVP was firstly studied using FT-IR.

FT-IR spectra of pure amorphous BMS-817399, PVP K30, ASDs, and physical mixtures (PM) with different drug loadings were acquired. As shown in Figure 2a, the 2 peaks centered at 1612 and 1667 cm^{-1}, indicated by the dash lines, was assigned to the carbonyl group of pure amorphous BMS-817399 and pure PVPK30, respectively. In the spetra of PMs, there was no observable peak shift on the 2 carbonyl groups at each drug loading. By comparison, in the ASDs, with the decrease of drug loading, the peak centered at 1612 cm^{-1} assigned to the carbonyl group of BMS-817399 was blue-shifted while that assigned to the carbonyl moiety of PVP centered at 1667 cm^{-1} red-shifted (Fig. 2b), resulting in the formation of a broad peak with shoulder peak from 20% to 60% drug loadings, suggesting the formation of intermolecular interaction between amorphous BMS-817399 molecules and PVP in ASDs instead of PMs. However, the broad stretched peak assigned to the NH and OH group centered at 3360 cm^{-1} did not show significant shift in ASDs at different drug loading (data not shown). Intermolecular hydrogen bond between amide proton and carbonyl group in carbamido group was reported to form a pseudo 6-membered ring structure in some other compounds.[25] Thus, we reasoned that intermolecular interaction existed in amorphous drug molecules even in the absence of PVP, and when ASDs was formed, PVP disrupted the intermolecular interactions between BMS-817399 molecules themselves and formed hydrogen bonding with the −NH or −OH group of BMS-817399 through PVP carbonyl groups, resulting in the peak shifts on the carbonyl group instead of NH/OH group of drug molecules.

Drug-Polymer Interactions Investigated by Dynamic Vapor Sorption Under Low Relative Humidity

It was reported previously that the formation of drug-polymer interaction would deviate the amount of water absorption from the linear addition of the pure components.[19,26] Thus, we investigated the dynamic vapor sorption behavior of BMS-817399/PVP ASDs over a relatively low humidity range of 3%-33% RH, to confirm the existence of drug-polymer interaction while avoiding the risk of inducing phase separation. Indeed, all materials were confirmed to be amorphous after sorption experiment using PXRD and a single T_g using DSC (data not shown).

The water vapor sorption isotherms of pure amorphous BMS-817399, PVPK30, and ASDs with different drug loading were compared in Figure 3. Predicted isotherms for physical mixtures using linear addition of 2 components based on Equation 1 was also plotted, where W_{drug} and $W_{polymer}$ was the weight of water sorbed per unit weight of drug and polymer, respectively; m_{drug} and $m_{polymer}$ represented the weight fraction of drug and polymer in the system, assuming either component in the physical mixture will sorb water independently.

$$W_{predicted} = W_{drug}m_{drug} + W_{polymer}m_{polymer} \quad (1)$$

As shown in Figure 3, compared to the predicted water sorption values of physical mixtures, ASDs with the same drug loading exhibited significantly reduced amount of water vapor sorption. Similar phenomenon was reported by Zografi et al.[26] for indomethacin/PVP and ursodeoxycholic acid/PVP systems. It was proposed that the interaction between the drugs and PVP in the solid

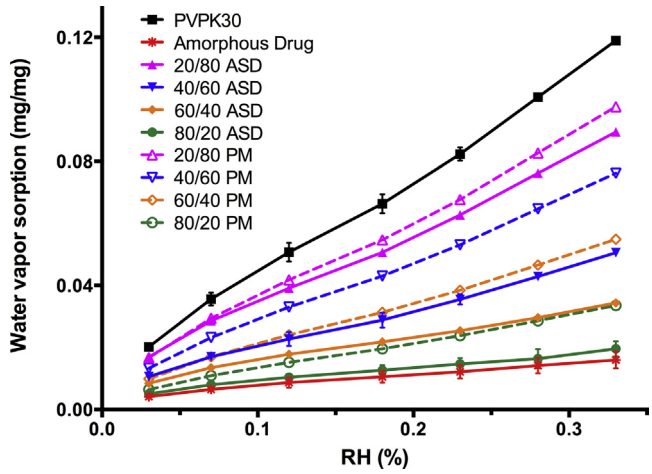

Figure 3. Water vapor sorption isotherms of ASDs, physical mixture, and pure components. The solid lines represented the isotherms of ASDs, whereas the dash lines with same color represented predicted isotherms of the physical mixtures with the same drug loading.

Table 1
BET Parameters of BMS-817399/PVP ASD Calculated Using Water Vapor Sorption Data

Material	Drug/PVP Ratio	W_m	C_B
PVP K30	NA	0.079 ± 0.008	9.4 ± 1.5
ASD	20/80	0.056 ± 0.002	12.1 ± 1.0
	40/60	0.030 ± 0.003	15.5 ± 1.4
	60/40	0.022 ± 0.001	17.8 ± 1.0
	80/20	0.013 ± 0.002	18.2 ± 1.8
PM	20/80	0.062[a]	10.9[a]
	40/60	0.048[a]	11.1[a]
	60/40	0.035[a]	11.5[a]
	80/20	0.021[a]	12.5[a]
Amorphous BMS-817399	NA	0.011 ± 0.002	16.0 ± 3.2

NA, not applicable.
[a] Value was calculated based on Equation 1.

dispersion could impede the ability of either drug or PVP to interact with water molecule by competition of hydrogen bonding sites.[26]

$$W = \frac{W_m C_B\,(p/p_0)}{[1-(p/p_0)][1-(p/p_0)+C_B(p/p_0)]} \quad (2)$$

To further reveal the physical nature of the drug-polymer interaction in the ASDs using the vapor sorption isotherms, BET equation (Eq. 2) was used to fit the isotherms, and the 2 invariables, W_m and C_B, was obtained (shown in Table 1). W_m, known as "monolayer limit," is the weight of water adsorbed corresponding to monolayer coverage, representing the number of sites available to form hydrogen bonding with water molecules on the material surface, whereas C_B represents the free energy of adsorption. It was shown that W_m increased with decreasing drug loading, whereas C_B showed an exactly opposite trend, since PVP is more hygroscopic than drug molecule. Also note that the calculated W_m value for physical mixture was significantly higher than that of ASDs with the same composition, suggesting hydrogen bonding formed between BMS-817399 and PVP in ASDs instead of physical mixture, and such interactions persisted within the tested RH range. C_B of physical mixtures was lower than that of ASDs at the same drug loading. Since C_B is affected by both the drug-polymer interaction and the free volume effects due to plasticizing,[16,26] it is too complicated to interpret C_B here with the limited information. Further experiments such as of dT_g/dw determination might facilitate a better interpretation of the C_B values.[16,26]

Amorphous Phase Separation Induced by High Relative Humidity

We further investigated the phase behaviors of BMS-817399/PVP ASDs on exposure to relatively high RH, when APS did occur. ASDs at different drug loading were exposed to 95% RH to reach equilibrium. XRD results confirmed ASDs still maintained amorphous after high moisture exposure (data not shown). Figure 2c showed the IR spectrum of ASDs after exposed to 95% RH to reach equilibrium. It was clearly seen that the peak centered at 1612 cm^{-1} assigned to the − C=O moieties of amorphous BMS-817399 arose in the spectra of ASDs caused by a red-shift after 95% RH exposure, indicating the disruption of drug-polymer interaction after moisture exposure.

We then specifically investigated the impact of different levels of moisture on the phase behavior of 40/60 ASD by DSC, FT-IR, and DVS. It was confirmed that the drug-polymer interaction did persist under 33% RH since the water vapor sorption isotherms was comparable for initial 40/60 ASD and ASD after being equilibrated at 33% RH and drying (Fig. 4c), and also no signs of APS were observed at 33% RH according to the IR spectra and the T_g measured (Figs. 4a and 4b). Disruption of drug-polymer interaction and initiation of APS started in the 40/60 ASD when the relative humidity reached 83% RH, demonstrated by the IR peak shift and the change of T_g.

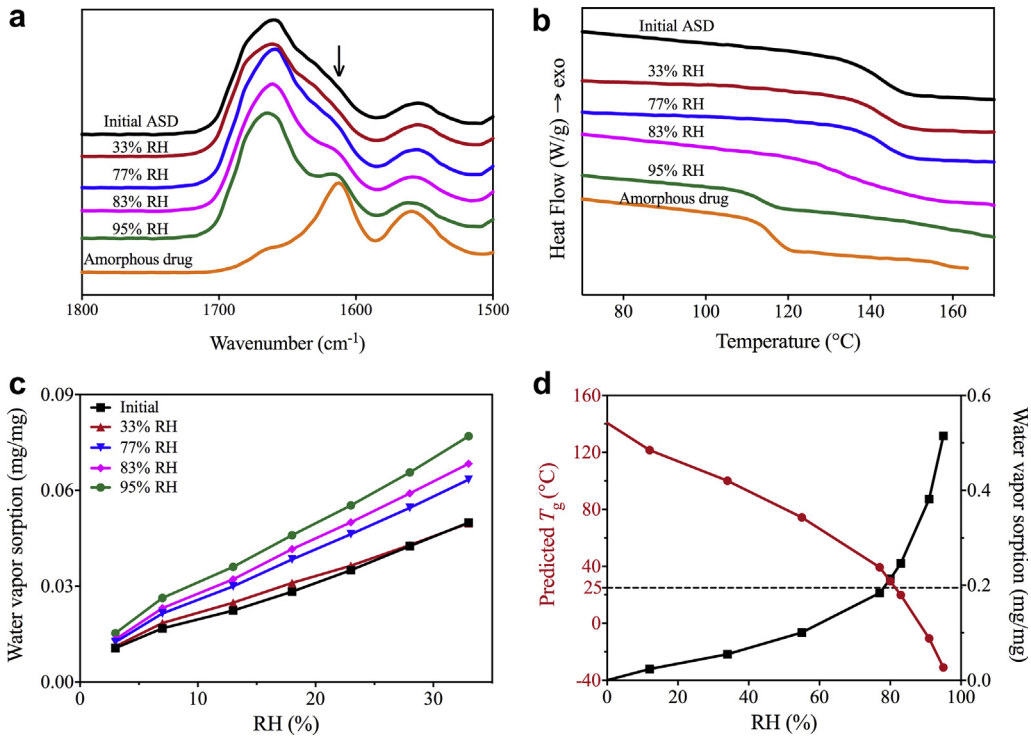

Figure 4. Phase separation behavior of 40/60 ASD after being exposed to different RH. (a), IR spectra of carbonyl group of 40/60 ASD; (b), modulated differential scanning calorimeter results of 40/60 ASDs and pure amorphous BMS-817399; (c), water vapor sorption isotherms of 40/60 ASD after first being equilibrated at different RH (d), the relationship between the amount of water vapor sorption and predicted Tg at different RH. The dash line in Figure 4d represented the temperature where water vapor sorption experiment was performed.

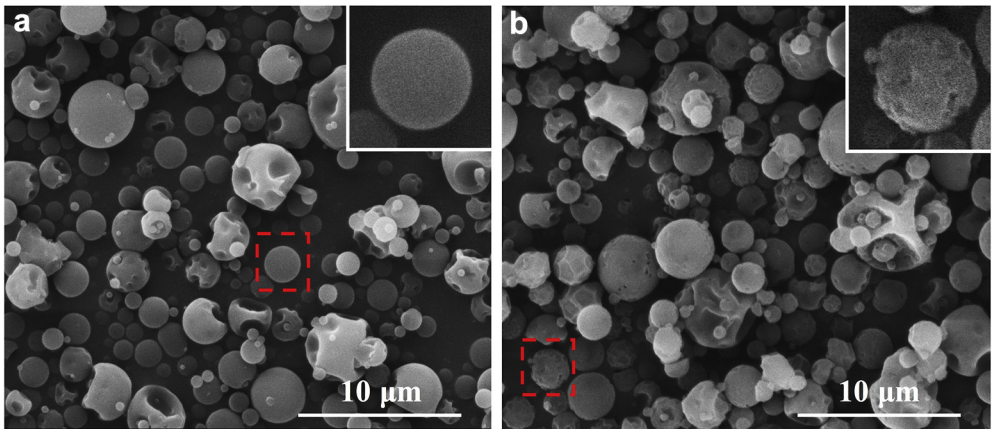

Figure 5. Surface morphology of 40/60 ASD powder before (a) and after (b) 95% RH (the right-top inset was a scale-up of the specific particle highlighted in red-dash square in the figure).

After exposure to 95% RH, the IR peak assigned to carbonyl group of amorphous BMS-817399 in 40/60 ASD shifted back and a T_g consistent with pure amorphous BMS-817399 was detected, indicating an complete amorphous phase separation. It is worth noting that, DSC detectable phase separation only occurred when ASDs were equilibrated under relative humidity higher than 83% RH. With the reported T_g value of water as 134 K (−139°C),[27] we estimated the T_g of the vapor equilibrated ASDs at each RH using Fox's equation (Fig. 4d). It was found that the 83% RH happened to be the cutoff RH where the ASD water content could lower the T_g to 293 K, below the experimental temperature (298 K). At the same time, it is also worth pointing out that, below the 83% RH cutoff when macroscopic APS was not detectable by DSC (77% RH), the amount of water vapor sorption by ASDs did elevate after being exposed to moisture (Fig. 4c). As mentioned earlier, a higher water vapor sorption suggested partial disruption of drug-polymer interactions thus more water binding sites were exposed to moisture (Fig. 3).

The above results suggested 2 roles of water during moisture-induced APS: (1) disruption of the drug-polymer interactions, and (2) plasticizing of the ASD to increase the molecular mobility and accelerate the APS. Generally, it is difficult to distinguish the contribution of these 2 effects of water molecules on the phase separation. In the case of BMS-817399/PVP ASD, it seems to demonstrate that both mechanisms exist and both are crucial for the occurrence of APS that became significant enough to be visible by DSC (i.e., ~30-nm scale[28]). For ASDs without detectable change of T_g after moisture exposure below 83% RH, the change in the water vapor sorption might be indicating nano-scale phase separation, which could not be detected by DSC or IR spectra. Other supplemental tools such as nano-IR spectroscopy[29] and solid state NMR,[30] may be helpful in revealing a more subtle APS.

Surface Morphology and Chemical Composition of ASDs After Amorphous Phase Separation

To determine if APS would cause any morphological changes on the spray-dried ASD particles, surface morphology of 40/60 ASD before and after 95% RH moisture exposure was visualized by scanning electron microscopy. Hollow central void particles were reported for BMS-817399 with 90.9% drug loading prepared by spray drying.[31,32] In our 40/60 ASD system, central void particles, as well as spherical particles with a relatively wide distribution of particle size were observed for freshly-made ASD. After 95% RH exposure, there were less spherical particles with fine and smooth surface; instead, more particles with irregular shape, porous and rough surface were observed (Fig. 5). Apart from this, no particle aggregation and other significant visible difference were observed on the surface morphology and average particle size of ASD before and after 95% RH exposure.

Although no major morphological changes were observed after APS, the surface chemical composition of the ASDs changed dramatically, as characterized by XPS. Figure 6 shows XPS spectra collected for 40/60-ASD before and after 95% RH exposure, respectively. There are 2 peaks in the spectra, corresponding to the photoelectrons from the nitrogen atom (N) and chlorine atom (Cl), respectively. Since Cl is only presented in the drug molecule, whereas both drug and PVP contain N atoms, the ratio of the 2 peak

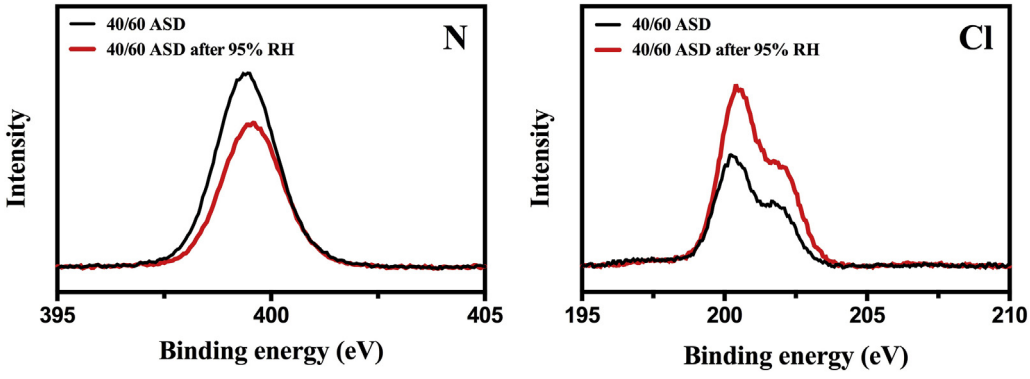

Figure 6. N1s and Cl2p XPS spectra of BMS-817399/PVP-40/60-ASD before and after 95% RH exposure.

Table 2
Fraction of Drug on the Surface of 40/60 ASD Before and After Moisture Exposure

Material	Atomic %		Drug wt %
	Cl	N	
Initial 40/60-ASD	1.4	13.3	39
40/60-ASD after 95% RH	2.5	12.4	69

areas, $x_{Cl/N}$, can then be used to calculate the surface concentration of drug by the following equation:

$$w_{drug} = 100\% \times x_{Cl/N} M_{drug} \Big/ \left[x_{Cl/N} M_{drug} + \left(1 - 3x_{Cl/N}\right) M_{PVP} \right] \quad (3)$$

where w_{drug} is the drug weight percentage on the surface, and M_{drug} and M_{PVP} are respectively the molar masses of NMP and the repeat unit of polymer's repeating unit (111 g/mol for PVP). The calculated drug on the surface was shown in Table 2. It was shown that the freshly prepared 40/60 ASD particles have a surface drug composition very similar to the theoretical bulk value of 40%. However, after exposed to 95% RH to induce APS, the ASD surface drug concentration increased to 69%. Since BMS-817399 is a hydrophobic drug, it is reasonable that the drug molecules tended to diffuse to the solid-air interface after phase separation initiated. This phenomenon suggested that the moisture-induced phase separation on the micro-scale could be nonhomogeneous, resulting in different composition on the surface and in the bulk. Drug-rich surface caused by phase separation could have an impact on either the physical stability or dissolution performance of ASD. Recent progress in understanding the role of surface mobility in glasses and its importance on the physical stability has revealed that surface diffusion in molecular glasses can be 10^6-10^8 times faster than bulk diffusion, which enables fast crystal growth on the free surface.[33-36] Therefore, when drug concentrated onto the surface, crystallization could be accelerated since the concentration of drug on the surface increased and meanwhile there is less polymer encompassing to prevent the crystallization of amorphous drug by drug-polymer interaction. The influence of such change of spatial distribution on dissolution performance of ASD is also certainly worth investigation, which will be discussed in detailed in the next section.

The Impact of Amorphous Phase Separation on the Dissolution Performance

The occurrence of APS in ASD could affect its dissolution performance due to several mechanisms: (1) the emerging of drug-rich and polymer-rich regions in the ASD could affect the dissolution rate of drug molecules from ASD matrix due to their changed immediate neighboring environment; (2) the crystallization inhibitory effect by polymers in water-sorbed ASDs could be different; (3) the change of surface chemistry and surface hydrophobicity could affect the wettability and dispersity of ASDs in dissolution medium; (4) disruption of drug-polymer interactions could also jeopardize the supersaturation of the drug, which could otherwise be prolonged. Therefore, we firstly compared the intrinsic dissolution rate (IDR) of 40/60 BMS-817399/PVP ASDs, before and after APS. As an additional control, we also determined the IDR of a physical mixture mixing by 20/80 ASD and 60/40 ASD with an overall drug/polymer ratio of 40/60 as well.

The drug and polymer release profiles were shown in Figures 7a and 7b, whereas the calculated IDR were shown in Figure 7c. To our surprise, there was no significant alteration on the drug release after moisture-induced phase separation, whereas polymer release was only moderately but significantly slowed down compared with initial ASD, although APS was confirmed doubtlessly by DSC, XPS, and FT-IR.

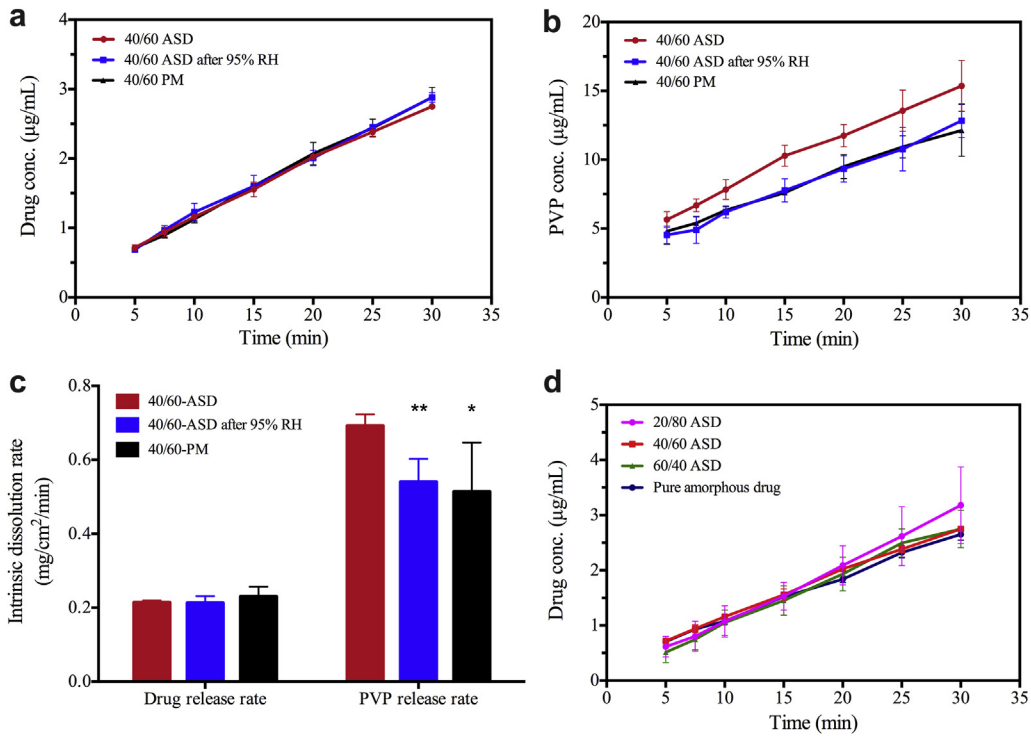

Figure 7. Drug (a) and polymer (b) release from BMS-817399/PVP-40/60-ASD before and after 95% RH exposure and 40/60-PM, calculated intrinsic dissolution rate (c) ($^{*}p$ <0.05, $^{**}p$ <0.01) and drug release from pure amorphous drug and ASD at different drug loadings (d).

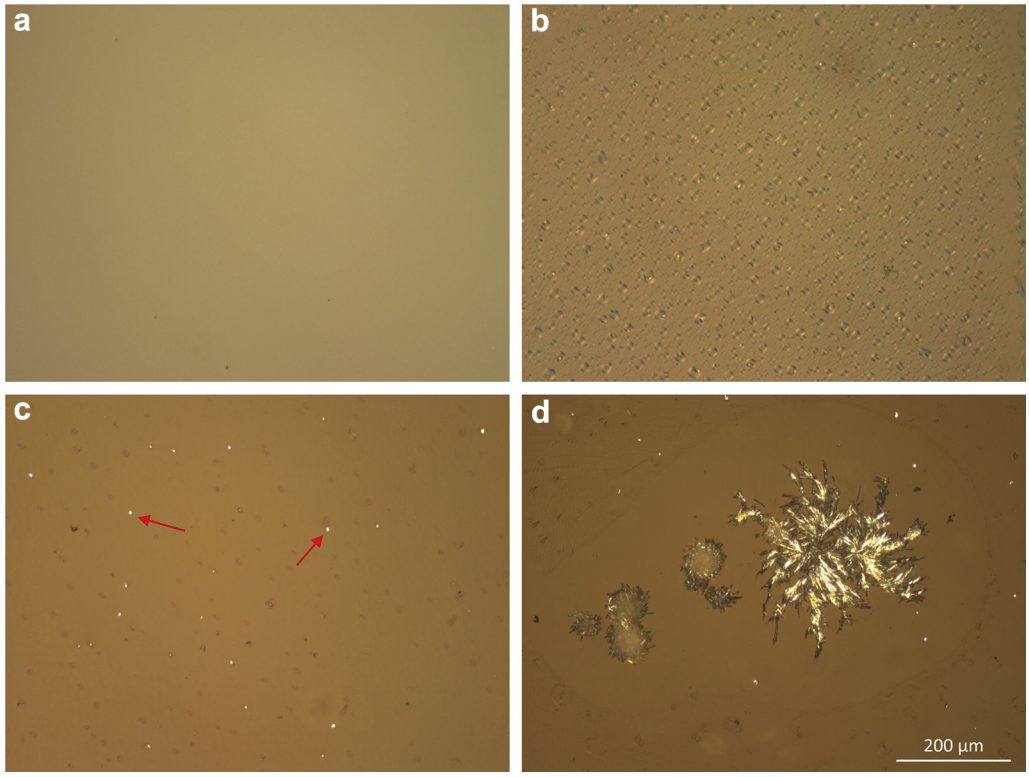

Figure 8. Crystallization kinetics of amorphous BMS-817399 film before moisture exposure (a) and after storage at 97% RH for 12 h (note: dots in the picture were due to the shrinkage of the film when exposed to moisture) (b), 3 days (c) and 7 days (d).

In an earlier study, we reported that intrinsic dissolution rate of ASDs was significantly different from that of physical blends, based on the comparisons of ketoconazole (KTZ) ASD systems using PVP, PVPVA, or HPMC-AS as the polymer carriers.[23] We attributed these findings to a nonuniform molecular distribution of drug and polymer in physical mixture and the overall interaction strength.[23] With the presence of homogeneous mixing and specific drug-polymer interaction, drug and polymer dissolved at approximately the same rate from ASDs, whereas a nonhomogeneous mixing state and insufficient drug-polymer interaction resulted in slower drug dissolution rate compared with polymer release rate.[23]

However, in the current BMS-817399/PVP-40/60 ASD, polymer release rate was about 3 times of the drug release rate (0.77 vs. 0.21 mg/cm^2/min). A faster polymer release rate than drug release rate was also reported previously in KTZ/PVPK30 ASD with 40% drug loading regardless of the presence of drug-polymer interaction. In that case, the fast-dissolving PVPK30 was unable to carry sufficient amount of KTZ to achieve a comparable drug release rate owing to a weaker apparent drug-polymer interaction strength proved by FT-IR and NMR spectra.[23] In the case of BMS-817399/PVPK30-40/60 ASD, it is difficult to quantify the strength of apparent drug-polymer interaction based on FT-IR and water vapor sorption data, and the role of drug-polymer interaction plays on the dissolution rate was not conspicuous. In-depth studies are needed to identify the role of drug-polymer interaction as well as other factors participating in the dissolution process.

Besides the inconsistent release rate of drug and polymer in 817399/PVP-40/60 ASD, difference in the drug release rate between ASD and PM was not observed either, whereas polymer release rate in PM was found to be slower than that in ASD, similar as the KTZ/PVP system. To explain the phenomenon, we have conducted intrinsic dissolution for ASDs at multiple compositions. It was found that, the overall apparent dissolution rate (not normalized by drug loading) was similar for ASDs at all 3 drug loadings tested (Fig. 7d), which suggested that the normalized IDR of ASD was inversely proportional to the drug loading. Since the 40/60-PM was prepared by mixing 20/80-ASD and 60/40-ASD, it is conceivable that the apparent drug dissolution rate of PM was a combination of dissolution rate of the 2 components by linear superposition, which happened to be comparable to the dissolution rate of 40/60-ASD. However, the dissolution rate of polymers from 60/40-ASD decreased sharply to the detection limit of the ELSD (data not shown), which lead to a significantly lower overall polymer release rate from the PM between 20/80-ASD and 60/40-ASD, compared with the 40/60-ASD.

The drug and polymer dissolution rate of 40/60 ASD subjected to moisture-induced APS was also shown in Figure 7. It appeared that for the BMS-817399/PVP ASD system, regardless of the phase behavior and micro-/nano-scale spatial distribution of amorphous drug and PVP, the dissolution rate of amorphous BMS-817399 was hardly affected. We attributed this phenomenon to the extremely low crystallization tendency of amorphous BMS-817399, as well as an increased amount of surface drug due to APS.

Crystallization kinetics of amorphous BMS-817399 under 97% RH was monitored using PLM. No crystallization was detected within 12 h and only minimal crystal growth was observed after being stored for 3 days (Fig. 8). The extremely low crystallization propensity of amorphous BMS-817399 makes it a favorable model compound to study the amorphous phase separation behaviors of ASD on exposure to moisture, without the complication of drug recrystallization. Meanwhile, as a slower crystallizer, BMS-817399 crystallizes extremely slowly during dissolution process, even without the presence of PVP, thus crystallization kinetics was not considered as a crucial factor influencing the dissolution rate. For a phase-separated BMS-817399/PVP 40/60 ASD, decreasing polymer concentration on the surface and lack of drug-polymer interaction

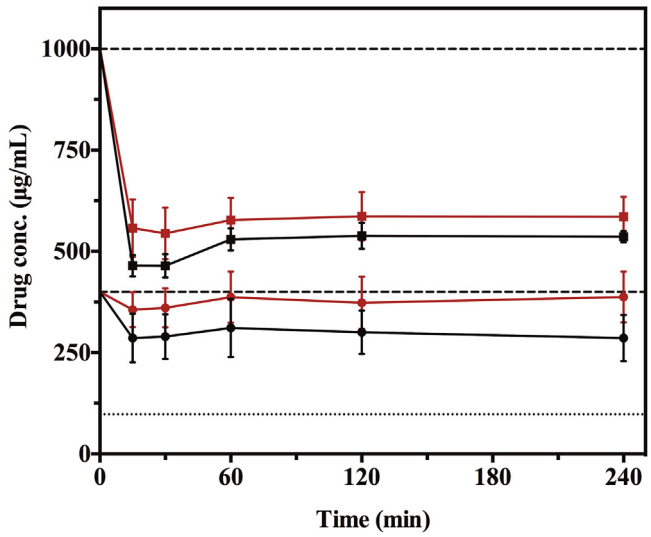

Figure 9. Supersaturation kinetics of BMS-817399 in PBS at ASD concentration of 0.4 mg/mL (circles) and 1 mg/mL (squares), with (red) or without (black) the presence of PVP K30, respectively. The dash line represents the initial supersaturation concentration, whereas the dot line indicates the crystalline solubility. The concentration of PVP was set to generate an initial BMS-817399/PVP concentration ratio of 40/60.

resulting from APS, will not lead to crystallization of amorphous drug at the beginning of dissolution process, thus may not affect the initial dissolution rate of drug.

In addition to the crystallization propensity, increased drug amount on the surface could also compromise on the dissolution rate. As discussed previously, in the presence of drug-polymer interaction, the fast-dissolving polymer could help improve the release of drug to achieve a comparable drug dissolution rate. If the drug-polymer interaction is disrupted, hydrophilic polymer was unable to help and the release rate of hydrophobic drug is expected to decrease. Accordingly, APS was expected to reduce the drug release rate. However, this was not observed in the phase-separated BMS-817399/PVP-40/60 ASD. To explain the phenomenon, we have also measured the IDR for pure amorphous drug at the same condition. It appeared that in the absence of drug-polymer interaction and poor wettability without polymers, the apparent drug dissolution rate, without normalized by drug loading, was similar to that of ASDs at different drug loadings, suggesting that the amount of drugs exposed to the dissolution medium was also one of the impact factors. Hence, even though the drug-polymer interaction was disrupted by moisture, the APS enriched surface drug might have compensated for the loss of drug-polymer interaction at the very beginning of dissolution process.

There is another explanation for the unchanged drug release rate after APS. It was suggested that ASD dissolution was governed by a competition between the dissolution rate and the rate of phase separation.[37,38] If APS was initiated immediately when BMS-817399 ASD came in contact to the dissolution medium, the difference between an originally homogeneous ASD and a phase-separated ASD may not be distinguishable by the intrinsic dissolution rate, but this theory cannot explain the decreased polymer release rate after phase separation.

The phenomenon that the polymer release rate decreased after phase separation could be attributed to the formation of a drug-rich surface resulting from APS, which gave rise to lower PVP concentration on the surface of the ASD. The reduced polymer release rate could result in a lower PVP concentration in the dissolution media, which may not be adequate to effectively inhibit drug precipitation or prolong the supersaturation maintenance. To evaluate the influence of APS on the supersaturation maintenance, supersaturation kinetics of BMS-817399 with or without the presence of PVP was assessed to determine the ability of PVP to maintain BMS-817399 supersaturation in aqueous environment. Solubility of crystalline BMS-817399 in 50-mM PBS with 0.5% dimethyl sulfoxide was determined to be 98 μg/mL. As shown in Figure 9, in the absence of PVP, the concentration of BMS-817399 decreased rapidly from the initial 1 mg/mL (i.e., ~10 times supersaturation) to 464 μg/mL within 15 min, and then slightly increased to ~530 μg/mL in 60 min. The supersaturation concentration was about 5 times of the crystalline solubility in the dissolution media and was maintained over the following 3 h. With the presence of 1.5-mg/mL PVP, the supersaturation was slightly improved and a concentration about 6 times crystalline solubility (~580 μg/mL) was achieved and maintained. When decreasing the initial BMS-817399 concentration to 0.4 mg/mL (i.e., ~4 times supersaturation), drug supersaturation was also slightly improved over 4 h with the presence of PVP. Overall, for a slow crystallizer like BMS-817399, PVP appeared to have very limited ability to prevent the precipitation of highly supersaturated BMS-817399 in the dissolution media. Therefore, despite of decreased PVP concentration in the dissolution media due to slower initial dissolution rate of PVP after APS, supersaturation maintenance is not anticipated to be significantly altered in a phase-separated BMS-817399/PVP-40/60 ASD. To conclude, phase separation will not have any significant effects on either the initial dissolution rate or the supersaturation maintenance of BMS-817399 in BMS-817399/PVP 40/60 ASD.

Conclusion

The potential risk of APS is high for ASDs composed of a hydrophobic drug and a hydrophilic polymer, particularly when the ASDs were exposed to moisture. The water sorption from the environment could destroy the drug-polymer interaction and significantly increase the molecular mobility, thus lead to immiscibility, and further, APS when the molecular mobility becomes high enough. The moisture-induced APS may not always have any substantial impacts on the dissolution performance of ASD, especially when the drug is a slow crystallizer like BMS-817399. Therefore, for such slow crystallizers, amorphous solid dispersion could be a relatively low risk formulation approach not only because of the low risk of drug recrystallization but also because the potential APS could only have minimal impact on the dissolution performance. Considering these aspects, drug loading of ASD containing slow crystallizers like BMS-817399 could be relatively high, as long as the PVP concentration could benefit the wettability and supersaturation maintenance. In fact, BMS-817399/PVP ASD with ~90% drug loading demonstrated satisfactory *in vivo* bioavailability in separate tests.

Compared with earlier studies, one message that should be conveyed is that, the dissolution performance of ASDs that undergo APS during manufacturing or storage could vary to different extents, depending on the hydrophobicity and crystallization propensity of the drug, drug-polymer interaction and various other factors. It is beneficial to obtain a more comprehensive micro-/nano-scale physical picture of the APS, thus to be able to evaluate the potential risks of dissolution performance and physical stability.

Acknowledgments

This research is supported by China National Nature Science Foundation (project number 81573355), and Bristol-Myers Squibb Company (Lawrenceville, NJ). FQ also thank the start-up funds provided by the Center for Life Sciences at Tsinghua and Peking

Universities (Beijing, China), and by the China Recruitment Program of Global Experts.

References

1. Singh A, Worku ZA, Van den Mooter G. Oral formulation strategies to improve solubility of poorly water-soluble drugs. *Expert Opin Drug Deliv*. 2011;8(10):1361-1378.
2. Vasconcelos T, Sarmento B, Costa P. Solid dispersions as strategy to improve oral bioavailability of poor water soluble drugs. *Drug Discov Today*. 2007;12(23-24):1068-1075.
3. Brough C, Williams 3rd RO. Amorphous solid dispersions and nano-crystal technologies for poorly water-soluble drug delivery. *Int J Pharm*. 2013;453(1):157-166.
4. The use of amorphous solid dispersions: a formulation strategy to overcome poor solubility and dissolution rate. *Drug Discov Today Technol*. 2012;9(2):e71-e174.
5. Hancock BC, Zografi G. Characteristics and significance of the amorphous state in pharmaceutical systems. *J Pharm Sci*. 1997;86:1-12.
6. Serajuddin ATM. Solid dispersion of poorly water-soluble drugs: early promises, subsequent problems, and recent breakthroughs. *J Pharm Sci*. 1999;88:1058-1066.
7. Qian F, Huang J, Hussain MA. Drug-polymer solubility and miscibility: stability consideration and practical challenges in amorphous solid dispersion development. *J Pharm Sci*. 2010;99(7):2941-2947.
8. Qian F, Huang J, Zhu Q, et al. Is a distinctive single Tg a reliable indicator for the homogeneity of amorphous solid dispersion? *Int J Pharm*. 2010;395(1-2):232-235.
9. Marsac PJ, Rumondor AC, Nivens DE, Kestur US, Stanciu L, Taylor LS. Effect of temperature and moisture on the miscibility of amorphous dispersions of felodipine and poly(vinyl pyrrolidone). *J Pharm Sci*. 2010;99(1):169-185.
10. Rumondor AC, Wikstrom H, Van Eerdenbrugh B, Taylor LS. Understanding the tendency of amorphous solid dispersions to undergo amorphous-amorphous phase separation in the presence of absorbed moisture. *AAPS PharmSciTech*. 2011;12(4):1209-1219.
11. Rumondor ACF, Marsac PJ, Stanford LA, Taylor LS. Phase behavior of poly(vinylpyrrolidone) containing amorphous solid dispersions in the presence of moisture. *Mol Pharm*. 2009;6:14.
12. Rumondor ACF, Taylor LS. Effect of polymer hygroscopicity on the phase behavior of amorphous solid dispersions in the presence of moisture. *Mol Pharm*. 2010;7:477-490.
13. Vasanthavada M, Tong W-Q, Joshi Y, Kislalioglu MS. Phase behavior of amorphous molecular dispersions II: role of hydrogen bonding in solid solubility and phase separation kinetics. *Pharm Res*. 2005;22(3):440-448.
14. Hancock BC, Zografi G. The relationship between the glass transition temperature and the water content of amorphous pharmaceutical solids. *Pharm Res*. 1994;11:471-477.
15. Mehta M, Kothari K, Ragoonanan V, Suryanarayanan R. Effect of water on molecular mobility and physical stability of amorphous pharmaceuticals. *Mol Pharm*. 2016;13(4):1339-1346.
16. Zhang J, Zografi G. The relationship between "BET"- and "free volume"-derived parameters for water vapor absorption into amorphous solids. *J Pharm Sci*. 2000;89:1063-1072.
17. Bhugra C, Pikal MJ. Role of thermodynamic, molecular, and kinetic factors in crystallization from the amorphous state. *J Pharm Sci*. 2008;97(4):1329-1349.
18. Yu L. Amorphous pharmaceutical solids: preparation, characterization and stabilization. *Adv Drug Deliv Rev*. 2001;48:27-42.
19. Chen Y, Liu C, Chen Z, et al. Drug-polymer-water interaction and its implication for the dissolution performance of amorphous solid dispersions. *Mol Pharm*. 2015;12(2):576-589.
20. Ilevbare GA, Liu H, Edgar KJ, Taylor LS. Maintaining supersaturation in aqueous drug solutions: impact of different polymers on induction times. *Cryst Growth Des*. 2013;13(2):740-751.
21. Paudel A, Worku ZA, Meeus J, Guns S, Van den Mooter G. Manufacturing of solid dispersions of poorly water soluble drugs by spray drying: formulation and process considerations. *Int J Pharm*. 2013;453(1):253-284.
22. Vasanthavada M, Tong W-Q, Joshi Y, Kislalioglu MS. Phase behavior of amorphous molecular dispersions I: determination of the degree and mechanism of solid solubility. *Pharm Res*. 2004;21(9):1598-1606.
23. Chen Y, Wang S, Wang S, et al. Initial drug dissolution from amorphous solid dispersions controlled by polymer dissolution and drug-polymer interaction. *Pharm Res*. 2016;33(10):2445-2458.
24. Chen Y, Wang S, Wang S, et al. Sodium lauryl sulfate competitively interacts with HPMC-as and consequently reduces oral bioavailability of posaconazole/HPMC-as amorphous solid dispersion. *Mol Pharm*. 2016;13(8):2787-2795.
25. Yabuuchi K, Kato EMT. A new urea gelator: incorporation of intra- and intermolecular hydrogen bonding for stable 1D self-assembly. *Org Biomol Chem*. 2003;1:3464-3469.
26. Crowley KJ, Zografi G. Water vapor absorption into amorphous hydrophobic drug/poly(vinylpyrrolidone) dispersions. *J Pharm Sci*. 2002;91(10):2150-2165.
27. Masayasu S, Hiroshi S, Syûzô S. Calorimetric study of the glassy state. IV. Heat capacities of glassy water and cubic ice. *Bull Chem Soc Jpn*. 1968;41(11):2591-2599.
28. Krause S, Iskandar M. Phase separation in styrene-α-methyl styrene block copolymers. In: Klempner D, Frisch KC, eds. *Polymer Alloys. Polymer Science and Technology, vol 10*. Boston, MA: Springer; 1977:231-243.
29. Van Eerdenbrugh B, Lo M, Kjoller K, Marcott C, Taylor LS. Nanoscale mid-infrared imaging of phase separation in a drug-polymer blend. *J Pharm Sci*. 2012;101(6):2066-2073.
30. Yuan X, Sperger D, Munson EJ. Investigating miscibility and molecular mobility of nifedipine-PVP amorphous solid dispersions using solid-state NMR spectroscopy. *Mol Pharm*. 2014;11(1):329-337.
31. Gamble JF, Ferreira AP, Tobyn M, et al. Application of imaging based tools for the characterisation of hollow spray dried amorphous dispersion particles. *Int J Pharm*. 2014;465(1-2):210-217.
32. Gamble JF, Terada M, Holzner C, et al. Application of X-ray microtomography for the characterisation of hollow polymer-stabilised spray dried amorphous dispersion particles. *Int J Pharm*. 2016;510(1):1-8.
33. Cai T, Zhu L, Yu L. Crystallization of organic glasses: effects of polymer additives on bulk and surface crystal growth in amorphous nifedipine. *Pharm Res*. 2011;28(10):2458-2466.
34. Ishida H, Wu T, Yu L. Sudden rise of crystal growth rate of nifedipine near T(g) without and with polyvinylpyrrolidone. *J Pharm Sci*. 2007;96(5):1131-1138.
35. Lei Zhu LW, Yu L. Surface-enhanced crystallization of amorphous nifedipine. *Mol Pharm*. 2008;5(6):6.
36. Yu L. Surface mobility of molecular glasses and its importance in physical stability. *Adv Drug Deliv Rev*. 2016;100:3-9.
37. Raina SA, Alonzo DE, Zhang GG, Gao Y, Taylor LS. Using environment-sensitive fluorescent probes to characterize liquid-liquid phase separation in supersaturated solutions of poorly water soluble compounds. *Pharm Res*. 2015;32(11):3660-3673.
38. Ilevbare GA, Taylor LS. Liquid—liquid phase separation in highly supersaturated aqueous solutions of poorly water-soluble drugs: implications for solubility enhancing formulations. *Cryst Growth Des*. 2013;13(4):1497-1509.